

Available online at [www.sciencedirect.com](http://www.sciencedirect.com)

**jmr&t**  
Journal of Materials Research and Technology  
journal homepage: [www.elsevier.com/locate/jmrt](http://www.elsevier.com/locate/jmrt)



## Original Article

# A thermally stable and polarization insensitive square-shaped water metamaterial with ultra-broadband absorption



Yadgar I. Abdulkarim <sup>a</sup>, Halgurd N. Awl <sup>c</sup>, Fatih Ozkan Alkurt <sup>d</sup>,  
Fahmi F. Muhammadsharif <sup>e</sup>, Salah Raza Saeed <sup>a</sup>, Muharrem Karaaslan <sup>d</sup>,  
Mehmet Bakır <sup>f</sup>, Heng Luo <sup>b,\*</sup>

<sup>a</sup> Medical Physics Department, College of Medicals & Applied Science, Charmo University, 46023, Chamchamal, Sulaimania, Iraq

<sup>b</sup> School of Physics and Electronics, Central South University, Changsha, Hunan, 410083, China

<sup>c</sup> Department of Communication Engineering, Sulaimani Polytechnic University, 46001, Sulaimani, Iraq

<sup>d</sup> Department of Electrical and Electronics, Iskenderun Technical University, 31100, Hatay, Turkey

<sup>e</sup> Department of Physics, Faculty of Science and Health, Koya University, 44023, Koya, Iraq

<sup>f</sup> Department of Computer Engineering, Bozok University, 66200, Yozgat, Turkey

## ARTICLE INFO

## Article history:

Received 24 January 2021

Accepted 19 May 2021

Available online 27 May 2021

## Keywords:

Water metamaterial

Perfect absorption

Ultra-band

Polarization independent

## ABSTRACT

In this paper, square-shaped water metamaterial is reported, which can be used as a perfect absorber for ultra-broadband absorption in the microwave frequency range. Computer Simulation Technology (CST) software was used to investigate the results numerically, while a 3D printing technology was used to fabricate the proposed design. The simulated and experimental results showed that the proposed structure achieved absorption of more than 90% in the frequency range from 10.4 to 30 GHz. Moreover, the proposed metamaterial-based system was able to show polarization insensitivity and to maintain a high absorption response in the temperature range from 0 to 100 °C, which revealed a good thermal stability. The absorption mechanism was elaborated taking into consideration the power loss, electric and magnetic field distributions at three resonant frequencies of 12.1, 17.5 and 24.97 GHz. The performance of the proposed system was seen to outperform that of the reported works in literature. It is believed that the metamaterial structure can be a good candidate for the application of energy harvesting and stealth technology due to the high absorption, thermal stability, low cost and easy fabrication of the proposed design.

© 2021 The Author(s). Published by Elsevier B.V. This is an open access article under the CC BY-NC-ND license (<http://creativecommons.org/licenses/by-nc-nd/4.0/>).

\* Corresponding author.

E-mail address: [luohengcsu@csu.edu.cn](mailto:luohengcsu@csu.edu.cn) (H. Luo).

<https://doi.org/10.1016/j.jmrt.2021.05.031>

2238-7854/© 2021 The Author(s). Published by Elsevier B.V. This is an open access article under the CC BY-NC-ND license (<http://creativecommons.org/licenses/by-nc-nd/4.0/>).

## 1. Introduction

The artificially modified and periodic electromagnetic meta-materials have been well utilized in numerous important applications such as antenna technologies [1–4], radar [5–7], imaging systems [8–12] and microwave absorber [13–16]. The principle of meta-material theory is based on creating exotic electromagnetic behaviors that are not commonly found in natural materials when electromagnetic waves are exposed to them [17,18]. With this exotic behavior, the meta-material and its engineered medium would show a negative permittivity, negative permeability and negative refractive index, thereby modifying the interaction of electromagnetic waves [19].

Meta-materials have been widely used to improve the absorption response at specified frequencies. For instance, sandwich-shaped structures were utilized to form a metal–dielectric-metal layer [6,7,12–14]. In the sandwich configurations, the incident electromagnetic wave can be confined between the resonators, and hence leading to the absorption of the electromagnetic wave. In recent years, water based meta-material configurations have received considerable attention by researchers [20–27]. In a study [20], researchers proposed a tunable meta-material absorber incorporating a substrate layer of water, thereby taking benefit from the dispersive permittivity of water in the microwave region, especially in the frequency band of 4–20 GHz. In another study, Yoo et al. reported an electromagnetic meta-material absorber which used water droplets to create nearly perfect absorption characteristics in the frequency range of 8–18 GHz [21]. Moreover, Ren and Yin developed an ultra-broad band microwave absorber, which is based on cylindrical water resonator. The proposed structure was able to establish a good absorption characteristic in the 5.5–24.2 GHz band [22]. On the other hand, a meta-material absorber was modelled by Xie et al., in which a water layer was used as substrate [23] to achieve absorption characteristics of nearly 90% in the frequency range of 12–29.6 GHz. Moreover, a novel meta-material absorber was designed to show flexible and ultra-wide band characteristics in the frequency range of 5.8–25.6 GHz [24]. Along this line, researchers investigated a three-dimensional water substrate meta-material structure, which has thermally tunable property in the frequency range of 8.3–21 GHz [25]. It was seen from literature that water can be injected into the dielectric layer of the meta-material [26] and that water droplets design [27] can create a broad band absorption in the microwave region of electromagnetic spectrum.

Motivated by the unique absorption feature of water in the microwave region, there is still room for the development and improvement of water-based metamaterials through considering different designs and shape confinement of the water molecules between specified substrates. Therefore, in this study, we present a novel meta-material design with a perfect absorption capability and ultra-broad band characteristics. The proposed meta-material absorber incorporates a water substrate layer with square unit cells. Because of water dispersive permittivity feature in the microwave region, the absorption band characteristic is interestingly improved. It was observed that the proposed absorber can be well operated

in a frequency range from 10 to 30 GHz. Moreover, the absorption performance was found to be nearly independent on the liquid phase temperature and the angle of polarization of the incident wave.

## 2. Simulation design of the ultra-broadband metamaterial absorber

The designed water-based metamaterials perfect absorber consists of four layers, as shown in Fig. 1(a). The first layer is made of silicon dioxide ( $\text{SiO}_2$ ) for its low cost, availability, very low moisture absorption and high thermal conductivity. The permittivity and thickness of the  $\text{SiO}_2$  layer are 3.9 and 2 mm respectively. The second layer of the proposed structure is made of water with a periodical square shape. The square shape is the hollow hole having a width and dimension of 2 mm. To make hollow square shapes inside the water layer PLA (Polylactic Acid) material was used. The PLA has permittivity of 3.5 with the same thickness of the water layer. A second layer of  $\text{SiO}_2$  was added onto the water layer with a thickness of 0.8 mm. The bottom layer of the whole design is made of copper, which acts as a ground plane to prevent the transmission of electromagnetic waves. The water is sandwiched between two layers of  $\text{SiO}_2$ , so the ground plane is the only metal layer. The water layer with square periodical holes is a metamaterial which provides double negative properties the extracted permittivity and permeability of the structure are negative, as shown in figure below. In the numerical simulation, the thicknesses of the metal plate and its electrical conductivity are 0.015 mm and  $5.8 \times 10^7$  S/m, respectively. In this work, the CST microwave studio numerical software was used to design the structure and to simulate the obtained results. Genetic algorithm was used to get optimized dimension of the proposed metamaterial.

As such, the optimal side length (P) of the square unit cells was found to be 18 mm. Closed boundary conditions have been applied on the unit cell in the x and y directions, while an open boundary was used in the z direction. This is because the electromagnetic wave is assumed to be x-polarized and propagated normal to the metamaterial in the positive z direction.

In this work, the electromagnetic wave is prevented to transmit through the whole structure due to the presence of the metal plane. Therefore, the absorptivity can be directly calculated from the reflection of the structure by using this equation,  $A = 1 - |S_{11}|^2$ . Where A is a loss and  $S_{11}$  is the reflection.

Debye formula can be used to describe the permittivity of water at radio frequency( $\omega$ ) [28] as follows:

$$\epsilon(\omega) = \epsilon_{\infty} + \frac{\epsilon_s - \epsilon_{\infty}}{1 - i\omega\tau} \quad (1)$$

where the room-temperature high-frequency permittivity is  $\epsilon_s = 78.4$ , static permittivity is  $\epsilon_{\infty} = 3.1$  and rotational relaxation time is ( $\tau$ ) =  $8.27 \times 10^{-12}$ s. To achieve a broadband absorption for the designed metamaterial absorber at room temperature, the proposed structure was optimized and its geometric parameters were numerically estimated by using genetic algorithm. As such, in order to realize a broadband

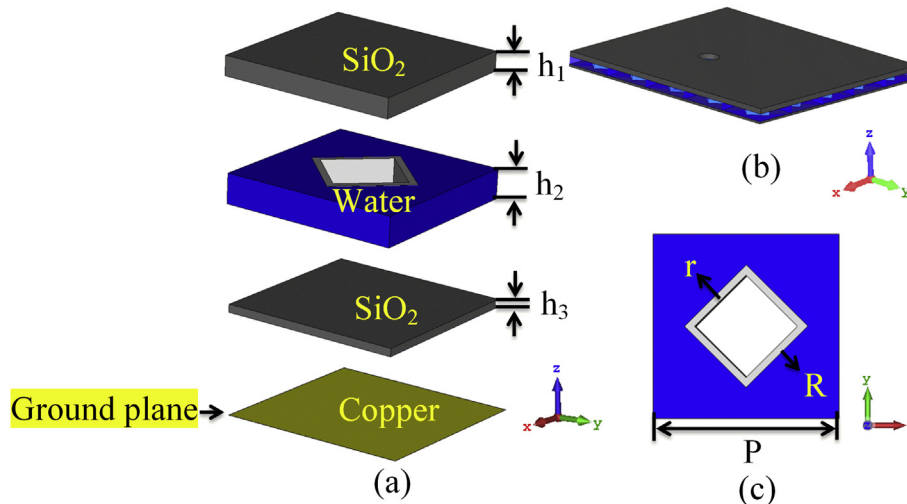


Fig. 1 – (a) The complete layers of the proposed unit cell structure, (b) The designed water metamaterials absorber and (c) front view of the water layer.

absorption of peak with more than 90%, the unit cell dimension of the water metamaterials was set to be  $18 \times 18$  mm.

### 3. Absorption results and field distributions

Figure 2 shows the simulation of the absorption spectra in the frequency range from 10 to 30 GHz for four different cases. As it can be seen from the graph, the optimized metamaterials absorber based on water can realize a high and broadband absorption within the desired frequency band. The proposed structure realized an absorptivity of more than 90% with their corresponding peaks at 12.1, 17.5 and 24.97 GHz.

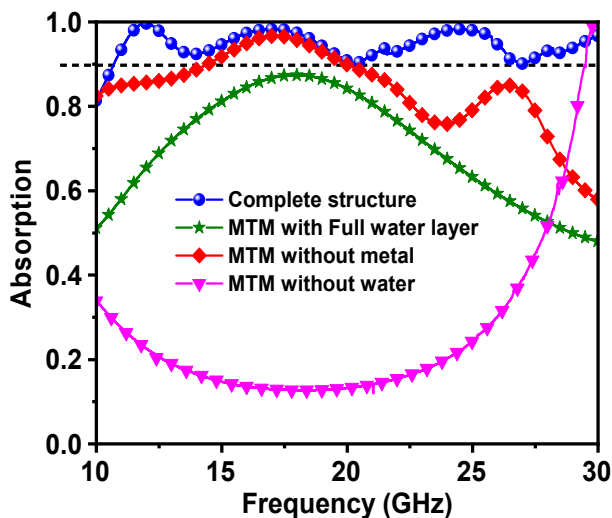


Fig. 2 – Simulated results of the absorptivity for the proposed metamaterials based on water under four different cases. The dotted horizontal line denotes the absorptivity of 90%.

The four cases are described as follows: in the first case, the metamaterial is unfilled with water layer and its absorptivity is recorded in the lower frequency range from 10 to 20 GHz. It was seen that the absorption peak has reached about 15%–34%, while it was gradually increased in the high frequency range. We observed in Fig. 2, the water layer as the dielectric resonator (DR) resonates at three different frequencies (12.1, 17.5, and 24.97 GHz) corresponding to three absorption peaks, while in the case of the structure without water layer no resonance peak has been observed, indicating that the water layer is responsible for producing resonance in the structure.

To physics behind the mechanism of resonance frequencies is attribute to the, the electric and magnetic distributions. Figs. 4 and 5 show a strong electric field with a weak magnetic field at the first and last resonance frequencies 12.1 GHz and 24.97 GHz for the studied structure. This indicates the strong electric resonances at these frequencies, while at the second resonance frequency where both electric and magnetic fields have relatively equal strength, meaning that both electric and magnetic field contributed to the resonance mechanism.

In the second case, we considered a full water layer without square holes, while the other parameters are kept constant. For several years, the dielectric resonator (DR) has primarily been used in different applications. In the studied case, due to the high permittivity water is considered as a DR. The resonant frequency is primarily determined by the size, shape, and material properties of the water. Therefore, in our design, the water layer behaves as a DR and produces a resonance frequency at 17.5 GHz. However, introducing the square hole in the water layer affects the properties of the resonance frequencies which leads to producing two more resonance frequencies and enhancing the absorption bandwidth. Hence, the broad absorption peak of the full water layer can be attributed to the frequency dispersive permittivity of water.

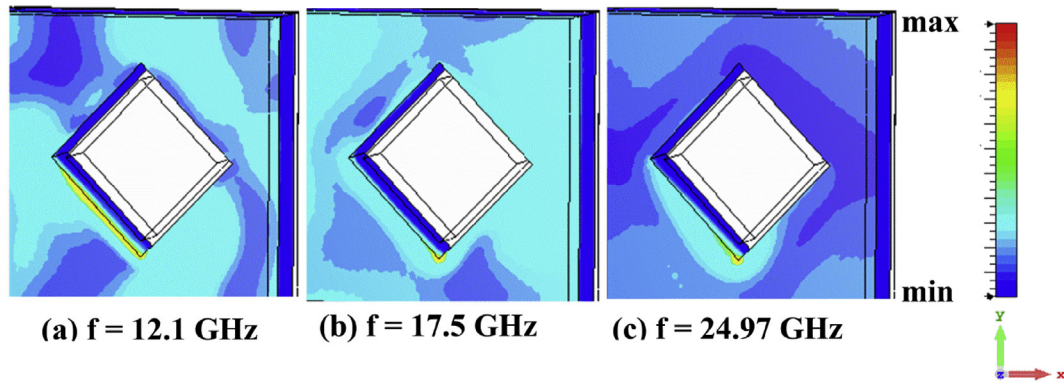


Fig. 3 – Simulated result of power loss densities of the water layer at (a) 12.1 GHz, (b) at 17.5 GHz and at (c) 24.97 GHz.

Noticeably, in the microwave frequency band, the water showed high absorption. The broadband absorption may be attribute to the intrinsic high loss of water. Comparably, the absorptivity of the metamaterial with full water was around 50%–89% in the desired frequency range, as shown in Fig. 2.

In the third case, the effect of metal ground layer on the absorptivity of the proposed structure was considered unlike metallic resonator-based metamaterial absorbers [29]. Results showed that in the low frequency range, from 13 to 21 GHz, the

absorptivity can surpass %90, while in the higher frequency range, the absorption performance is sharply declined.

Finally, the complete structure of the absorber, included square-shaped water metamaterial was investigated in the frequency range from 10.4 to 30 GHz. One can see, the proposed design shows a high absorptivity of more than 90% compared to that of the metal plane included. Noteworthy, higher absorptivities and a broadband absorption were achieved mainly due to the localized resonance in the metamaterial with the structured water resonators.

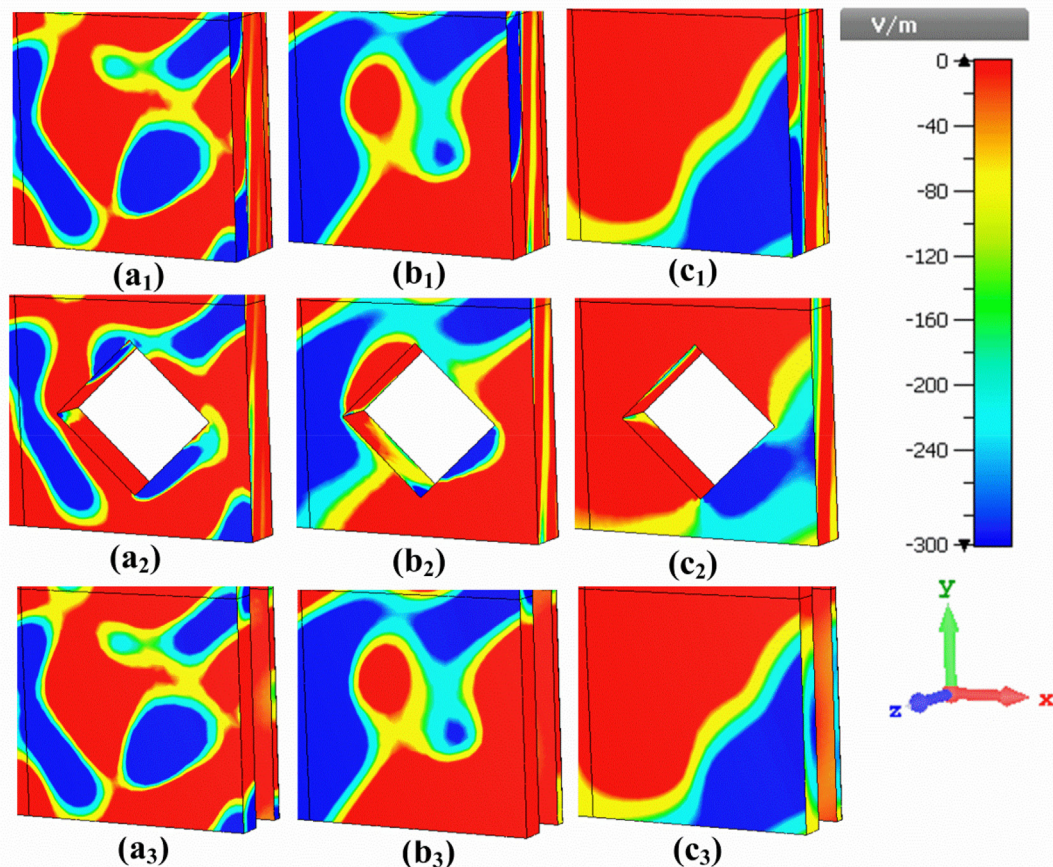


Fig. 4 – Electric Field distribution of the full structure (a<sub>1</sub>-c<sub>1</sub>), with water layer (a<sub>2</sub>-c<sub>2</sub>) and without water layer (a<sub>3</sub>-c<sub>3</sub>) at resonant frequencies of 12.1, 17.5 and 24.97 GHz, respectively.

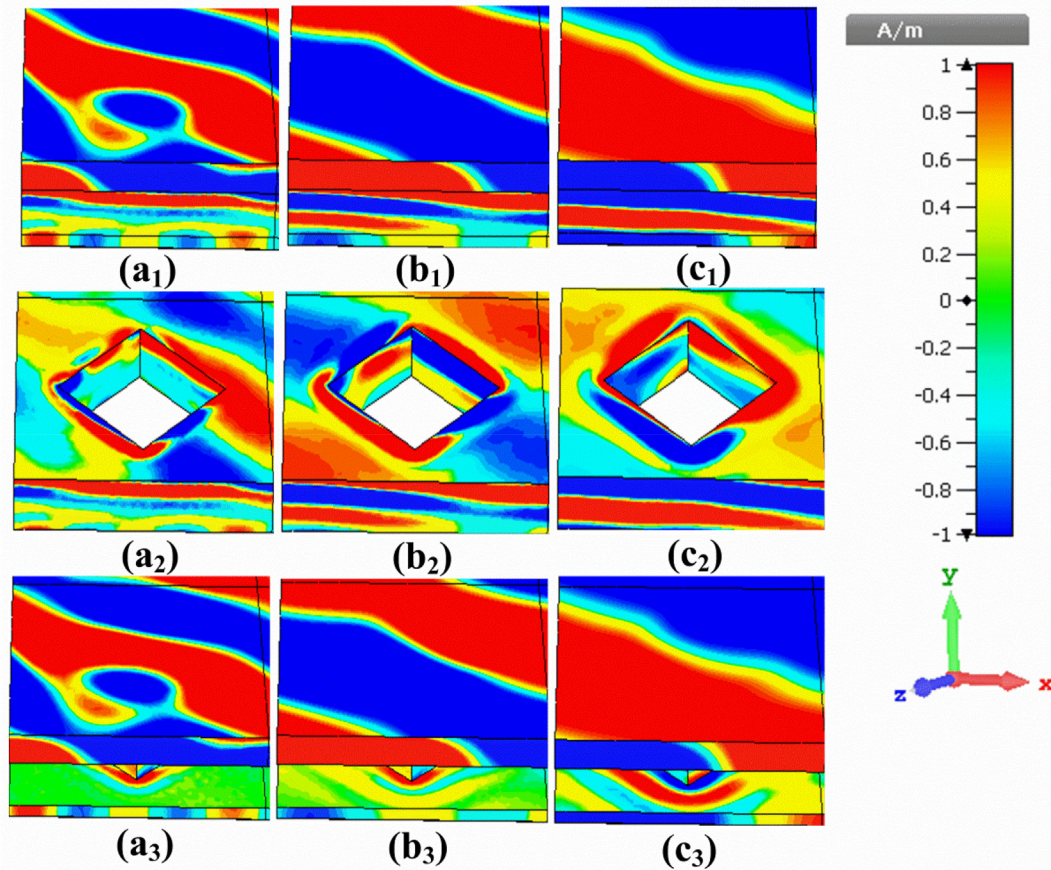


Fig. 5 – Magnetic field distribution of the full structure (a<sub>1</sub>-c<sub>1</sub>), with water layer (a<sub>2</sub>-c<sub>2</sub>) and without water layer (a<sub>3</sub>-c<sub>3</sub>) at resonant frequencies of 12.1, 17.5 and 24.97 GHz, respectively.

Figure 3 shows the distribution of power density loss across the water layer, where the absorption power loss is seen to be high around the square edges of the water metamaterial compared to that of the areas which are far from the square edges. Also, it was observed that the power density loss was decreased at the relatively high frequency of 25 GHz, while the largest power density loss was seen to be happened at the

resonant frequency of 17.5 GHz. This in turn led to achieving the maximum absorptivity along the spectrum of the proposed design, as can be seen in Fig. 2.

Figure 4 shows the electric field distribution across the proposed design with and without the presence of water

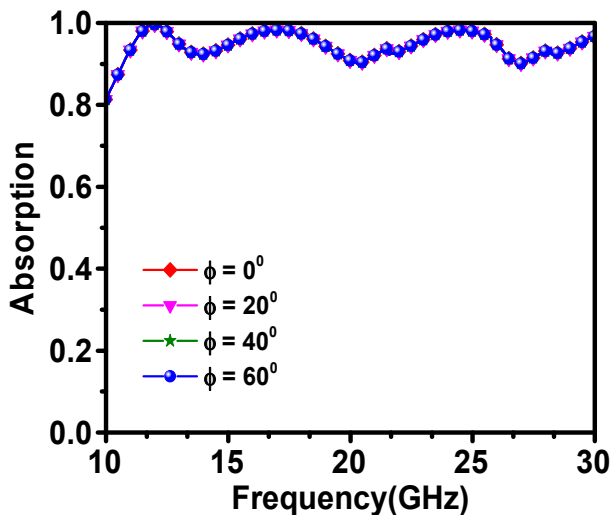


Fig. 6 – Polarization dependent of absorptivity.

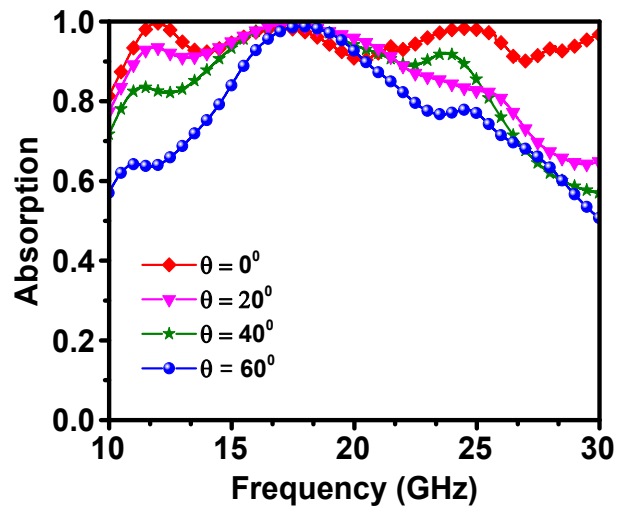
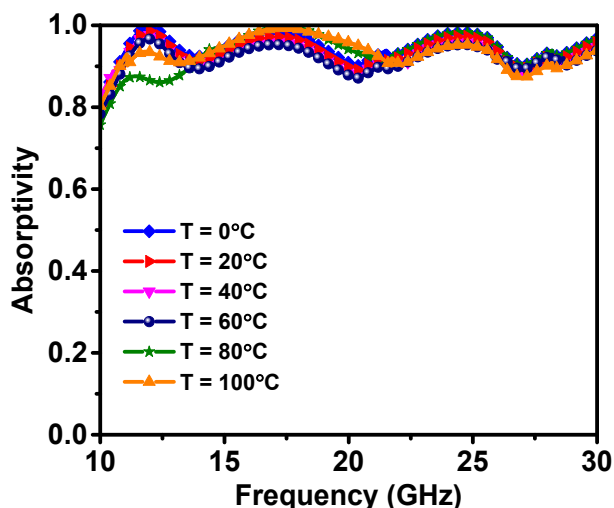


Fig. 7 – Absorptivity spectra of the proposed metamaterial absorber for oblique incidence waves with incident angle from 0 to 60° in the TE mode.



**Fig. 8 – Simulated absorptivity spectra at different temperatures, from 0 to 100 °C.**

metallayer at three different resonant frequencies. It was observed that the water square-shaped metallayer acted upon intensifying the electric field distribution, especially at the high resonant frequency of 24.97 GHz. Comparably, the structures without water metallayer presented a continuous distribution of low and high electric field densities, while the incorporation of water metallayer has made a disruption in the electric field. It was generally noticed that the electric field was highly confined along the square edges of the water metallayer, thereby improving the overall absorption response of the system, as was shown in Fig. 2.

Figure 5 shows the magnetic field distribution within the system with and without the presence of water metallayer at three different resonant frequencies. One can notice that the intensity of magnetic field is dependent on the resonant frequency, where a highly intensive magnetic field is generated across the center of the whole structure at 24.97 GHz. However, the addition of the water metallayer has led to relocate the magnetic field in the way that the square edges contributed to stabilize the magnetic field intensity, whereas most of

the intensive magnetic field was distributed along the edges of the square-shaped water metallayer.

#### 4. Polarization dependency, angular tolerance and thermal stability

In order to evaluate the performance of the proposed square-shaped water metamaterial absorber, the absorption under electromagnetic waves with different polarizations and incident angles were simulated. To simulate the polarization insensitivity under TE incidence, four different angles, namely 0°, 20°, 40° and 60°, were employed, as shown in Fig. 6. Noteworthy, because of the symmetric nature of the proposed design, the absorptivity remained unchanged from 10 to 30 GHz. Hence, as an absorber, the proposed structure, was able to adhere with the requirements of polarization angle independency.

Figure 7 shows the absorption dependency on the incident angle in TE mode. We further investigated the incident angle dependence of our proposed square-shaped absorber. The absorption spectra of the proposed structure was simulated, considering four different incident angles from 0° to 60° with a step size of 20° under TE polarization, as shown in Fig. 7. It is clear from Fig. 7 that the best absorptivity was observed at 0°. However, a perfect absorption was seen between 10.4 GHz and 30 GHz. When the incident angle was increased to 60°, the perfect absorption bandwidth was decreased to almost 25% of the total bandwidth. It should be noted that there is a significant difference in absorptivity between 0° and 60° incident angle, which can be understood from the working principle of the absorber. It is worth to mention that the magnetic dipole mode of the water resonator is excited. When the incident angle is set to 20°, the electric field is decreased and the dielectric resonators are getting weaker and weaker with the increase of incident angle. This in turn affects the bandwidth and perfect absorption frequencies directly hence the deviation in the absorption peaks and intensity are due to the decrease in the electric field under different incident angle of the wave in TE mode. However, the absorption is dependent on the incident angle, yet the structure presented a

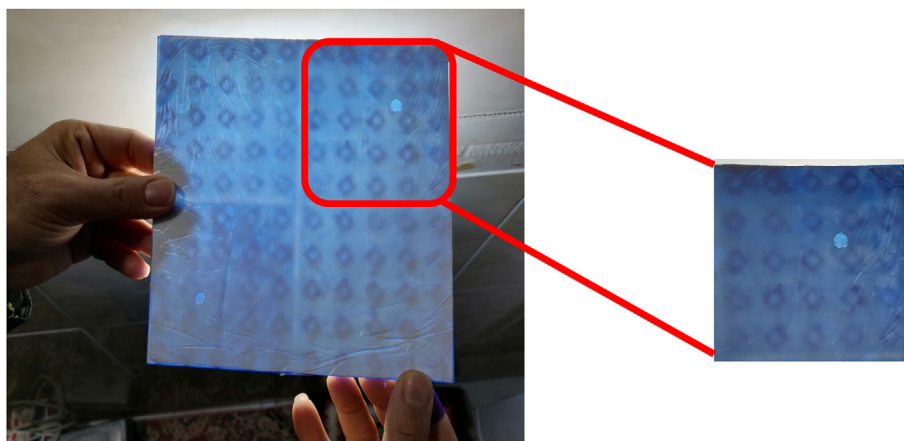


**Fig. 9 – Photos of the fabricated water metamaterial absorber consisting of 10 × 10 unit cells (left) and a substructure made of 5 × 5 arrays of unit cells (right).**

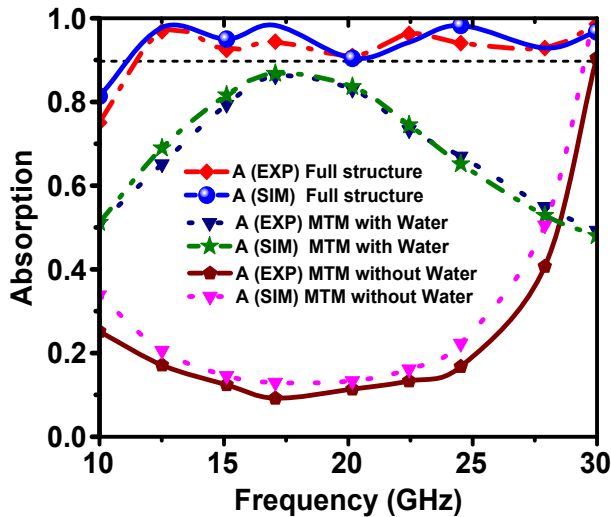


**Fig. 10 – Absorptivity results for the metamaterials based water under four different cases. (Experimental results).**

polarization-angle independency. The reason why our proposed structure is dependent on the angle of incidence wave but independent on the polarization angle can be referred to the nature of the square-shaped water metamaterial, which makes it to differently behave compared to those of literature.

Water is a temperature sensitive material whose dielectric constant and volume are changed with respect to the temperature. For this reason, the absorptivity should be investigated and elaborated under different temperatures. The dielectric constant of the water under different temperatures was predicted from Debye's formulas [28] and the material parameters were entered into the CST microwave studio. In order to verify the temperature dependency of the proposed structure, we have taken six different temperatures from 0 to 100 °C with a step size of 20 °C. It can be seen from Fig. 8 that the change in absorptivity with temperature is very small in the frequency range from 10 to 30 GHz. Absorptivity was slightly decreased at lower frequency but increased in the middle frequency band when the temperature was risen. Since the water container in the proposed structure was not sealed, for better practical applications, an external container

is recommended to prevent the performance degradation of the absorber due to thermal expansion (see Fig. 9).

## 5. Experimental results of the water metamaterial absorber

For the verification of the simulated results, the designed absorber was fabricated by utilizing a 3D printing technology. For this purpose, the frame of the structure was printed by the 3D printer with PLA (Polylactic Acid) material. The role of the PLA material frame is to keep molding the silicon. Then, the frame was removed and the fabricated structure remained as a hollow silicon container. The silicon container was then filled with water and a copper foil was added to the back side of the proposed structure, acting as a ground metal layer. Because of the limitation of sample size produced by the 3D printer, the designed  $10 \times 10$  array absorber was divided into four sub-structures of  $5 \times 5$ . The four fabricated sub-structures were adhered to the copper foil to get the fabricated absorber ready for measurement.

Figure 10 shows a comparison of the measured and numerical results of absorptivity for the water metamaterials absorber in four different cases. The measurements were performed by connecting the proposed structure to a broad band horn antenna via vector network analyzer in the room temperature. The reflectivity of the water metamaterial has been measured in the frequency range from 10 to 30 GHz. Then, by using the well-known equation,  $A = 1 - R$ , the absorptivity of the proposed structure was measured, as shown in Fig. 10. In our work, the value of transmission was neglected because of the back side of the proposed structure is made of total reflective copper plate. Both experimental and simulated results confirmed that the proposed water metamaterials absorber exhibited an ultra-broad band of up to 90% absorptivity in the frequency range of 10.4–30 GHz (full structure). It can be seen that the experimental and simulated results are in a good agreement with a small fluctuation in the results that may be due to the calibration of the vector network analyzer and manufacturing process.

To verify the achieved results, a fruitful comparison was made with the results of other works reported in literatures, in terms of absorber type, bandwidth absorptivity over 90% and the thickness of the water layer, as shown in Table 1.

**Table 1 – Comparison of the proposed water-based metamaterial with those reported in literature.**

References	Absorber type	Bandwidth (absorptivity over 90%) (GHz)	Thickness (mm)
[20]	Water-based absorber	6.2–19	3.5
[21]	Water-based absorber with periodic droplets	8–17	2
[22]	Cylinder-water-based absorber	5.58–24.1	3.8
[23]	Water-based absorber with cylindrical holes	12–29.6	5.8
[24]	Flexible water-based absorber	5.9–25.6	4
[25]	3D water-substrate array	8.3–21.0	15
[26]	Water - injected all - dielectric metamaterial	8.1–22.9	5.6
[27]	Water-tube metamaterial	5–15	7
This work	Water-based absorber with a square shape	10.4–30	2

## 6. Conclusions

In summary, a square-shaped water metamaterial perfect absorber was designed, fabricated and investigated successfully. The numerical and experimental results showed that the proposed structure achieved an ultra-broadband of more than 90% of absorptivity in the frequency range of 10.4–30 GHz. The study of temperature dependent absorption showed that the designed structure has a very good thermal stability, as well as it exhibited an excellent polarization-angle independent in the desired frequency range. It was seen that the simulated and experimental results are in a good agreement. The proposed water metamaterial can be easily fabricated to realize a low cost and real time use of its structure. We believe that the proposed structure can be a good candidate to be used in energy harvesting and stealth technology.

## Author contributions

Y.I.A. and H.N.A. conceived the idea; Y.I.A. and H.N.A. performed the simulations and performed the experiments; Y.I.A. and F.O.A. wrote the manuscript; F.F.M. M.B. and S.R.S. revised the manuscript; M.K.; Y.I.A. and H.L. supervised this research. All authors have read and agreed to the published version of the manuscript.

## Funding

This research was funding by the National Key Research and Development Program of China (Grant No. 2017YFA0204600), the National Natural Science Foundation of China (Grant No. 51802352), Central South University (Grant No. 2018zzts355) and Teaching reform for postgraduate students of Central South University (Grant No. 2019JG085).

## Data availability statement

No new data were created or analyzed in this study. Data sharing is not applicable to this article.

## Declaration of Competing Interest

The authors declared that they have no conflict of interest to this work.

## REFERENCES

- [1] Ali T, Pathan S, Biradar RC. Multiband, frequency reconfigurable, and metamaterial antennas design techniques: present and future research directions. *Internet Technol Lett* 2018;1(6):e19.
- [2] Hasan MM, Faruque MRI, Islam MT. Dual band metamaterial antenna for LTE/bluetooth/WiMAX system. *Sci Rep* 2018;8(1):1–17.
- [3] Sree MFA, Allam AMM. Design and fabrication of ultra-wideband leaky wave metamaterial antennas. *J Instrum* 2019;14(11):P11006.
- [4] Jiang M, Chen ZN, Zhang Y, Hong W, Xuan X. Metamaterial-based thin planar lens antenna for spatial beamforming and multibeam massive MIMO. *IEEE Trans Antenn Propag* 2016;65(2):464–72.
- [5] Brookner E. *Metamaterial advances for radar and communications*. 2017.
- [6] Baskey HB, Johari E, Akhtar MJ. Metamaterial structure integrated with a dielectric absorber for wideband reduction of antennas radar cross section. *IEEE Trans Electromagn C* 2017;59(4):1060–9.
- [7] Liu J, Li JY, Zhou SG. Polarization conversion metamaterial surface with staggered-arrangement structure for broadband radar cross section reduction. *IEEE Antenn Wireless Propag Lett* 2019;18(5):871–5.
- [8] Devadithya S, Pedross-Engel A, Watts CM, Landy NI, Driscoll T, Reynolds MS. GPU-accelerated enhanced resolution 3-D SAR imaging with dynamic metamaterial antennas. *IEEE Trans Microw Theor Tech* 2017;65(12):5096–103.
- [9] Imani MF, Gollub JN, Yurduseven O, Diebold AV, Boyarsky M, Fromenteze T, et al. Review of metasurface antennas for computational microwave imaging. *IEEE Trans Antenn Propag* 2020;68(3):1860–75.
- [10] Mukherjee S, Su Z, Udpa L, Udpa S, Tamburrino A. Enhancement of microwave imaging using a metamaterial lens. *IEEE Sensor J* 2019;19(13):4962–71.
- [11] Imani MF, Sleasman T, Smith DR. Two-dimensional dynamic metasurface apertures for computational microwave imaging. *IEEE Antenn Wireless Propag Lett* 2018;17(12):2299–303.
- [12] Alkurt FO, Altintas O, Atci A, Bakir M, Unal E, Akgol O, et al. Antenna-based microwave absorber for imaging in the frequencies of 1.8, 2.45, and 5.8 GHz. *Opt Eng* 2018;57(11):113102.
- [13] Yu P, Besteiro LV, Huang Y, Wu J, Fu L, Tan HH, et al. Broadband metamaterial absorbers. *Adv Opt Mater* 2019;7(3):1800995.
- [14] Zhou Q, Yin X, Ye F, Mo R, Tang Z, Fan X, et al. Optically transparent and flexible broadband microwave metamaterial absorber with sandwich structure. *Appl Phys A* 2019;125(2):131.
- [15] Sim MS, You KY, Esa F, Dimon MN, Khamis NH. Multiband metamaterial microwave absorbers using split ring and multiwidth slot structure. *Int J RF Microw Computer-Aided Eng* 2018;28(7):e21473.
- [16] Alkurt FÖ, Altıntaş O, Bakir M, Karaaslan M, Ünal E, Karadag F, et al. Microwave power imaging detector based on metamaterial absorber. *Opt Eng* 2020;59(8):087104.
- [17] Veselago V, Braginsky L, Shklover V, Hafner C. Negative refractive index materials. *J Comput Theor Nanosci* 2006;3(2):189–218.
- [18] Schurig D, Mock JJ, Justice BJ, Cummer SA, Pendry JB, Starr AF, et al. Metamaterial electromagnetic cloak at microwave frequencies. *Science* 2006;314(5801):977–80.
- [19] Smith DR, Pendry JB, Wiltshire MC. Metamaterials and negative refractive index. *Science* 2004;305(5685):788–92.
- [20] Pang Y, Wang J, Cheng Q, Xia S, Zhou XY, Xu Z, et al. Thermally tunable water-substrate broadband metamaterial absorbers. *Appl Phys Lett* 2017;110(10):104103.
- [21] Yoo YJ, Ju S, Park SY, Kim YJ, Bong J, Lim T, et al. Metamaterial absorber for electromagnetic waves in periodic water droplets. *Sci Rep* 2015;5:14018.
- [22] Ren J, Yin JY. Cylindrical-water-resonator-based ultra-broadband microwave absorber. *Opt Mater Express* 2018;8(8):2060–71.



- 
- [23] Xie J, Zhu W, Rukhlenko ID, Xiao F, He C, Geng J, et al. Water metamaterial for ultra-broadband and wide-angle absorption. *Opt Express* 2018;26(4):5052–9.
- [24] Wu Z, Chen X, Zhang Z, Heng L, Wang S, Zou Y. Design and optimization of a flexible water-based microwave absorbing metamaterial. *APEX* 2019;12(5):057003.
- [25] Shen Y, Zhang J, Pang Y, Zheng L, Wang J, Ma H, et al. Thermally tunable ultra-wideband metamaterial absorbers based on three-dimensional water-substrate construction. *Sci Rep* 2018;8(1):1–10.
- [26] Huang X, Yang H, Shen Z, Chen J, Lin H, Yu Z. Water-injected all-dielectric ultra-wideband and prominent oblique incidence metamaterial absorber in microwave regime. *J Phys Appl Phys* 2017;50(38):385304.
- [27] Zhao J, Wei S, Wang C, Chen K, Zhu B, Jiang T, et al. Broadband microwave absorption utilizing water-based metamaterial structures. *Opt Express* 2018;26(7):8522–31.
- [28] Ellison W. Permittivity of pure water, at standard atmospheric pressure, over the frequency range 0–25 THz and the temperature range 0–100\_C. *J Phys Chem Ref Data* 2007;36:1–18.
- [29] Wang Yingying, Chen Zeqiang, Xu Danyang, Yi Zao, Chen Xifang, Chen Jian, et al. Triple-band perfect metamaterial absorber with good operating angle polarization tolerance based on split ring arrays. *Results Phys* 2020;16:102951.